

Along C^-

$$y_j - y_{j-1} = (x_4 - x_1) \tan(\theta_{14} - \mu_{14}) \quad (2a)$$

Along C^+

$$y_j - y_{j-1} = (x_4 - x_2) \tan(\theta_{24} + \mu_{24}) \quad (2b)$$

The computation of flow at a new grid point calls for either the semi-inverse marching algorithm (Fig. 3) or the inverse marching algorithm (Fig. 2), according to whether the particular grid point is located on an extension of a C^+ characteristic. In the code written to implement the SIMA scheme, C^+ characteristics were bypassed automatically when they approached the symmetry line ($x = 0$), and some inverse marching grid points were added between the symmetry line ($x = 0$) and the first C^+ characteristic.³

Thus, there are two types of new grid points in the SIMA scheme: the inverse marching type (Fig. 2) and the semi-inverse marching type (Fig. 3). In the inverse marching case, the location x_4 of a new point is determined in advance, and the trace points x_1, x_2 (Fig. 2) are obtained by inversely extending C^- and C^+ characteristics from new point (x_4, y_4) ; Eqs. (2) are used to get x_1 and x_2 . In the semi-inverse marching case (Fig. 3), the location of x_4 is obtained by a forward extension of C^+ from old point (x_2, y_2) , and trace point x_1 is obtained by an inverse extension of C^- from new point (x_4, y_4) ; again, Eqs. (2) are used for computing x_4 and x_1 .

The flow at each new grid point of either the inverse or the semi-inverse type is determined by solving the pair of implicit compatibility equations (1). The solution is obtained by iterations that are repeated at each point until convergence is established, the initial guess being given by the interpolated old grid flow variables. For more detailed information, the reader is referred to a report that also contains a plume code listing.³

Flow Test Case

As a test of the accuracy of the SIMA scheme, we chose the reflection of a PMF ($\delta = 0$) from a symmetry plane ($x = 0$), which represents a planar plume flow. The flow at $x = 0$ was independently computed by integrating the compatibility equations along characteristic lines fanning out from the corner and their reflections from the symmetry plane, using the direct method of characteristics.²

We have done so for the test case of $M_e = 3$, $\gamma = 1.4$, and a fan of C^+ lines chosen with $\Delta M = 0.05$ at the corner; it was verified by numerical convergence that $M(o, y)$ so obtained was practically an exact solution (relative error in Mach number of 10^{-5} or less). A SIMA computation was also performed for the same exit flow, and it is depicted in Fig. 4 (streamlines and lines of const M). The initial grid was comprised of 30 points across the exit plane (inverse points), followed by 30 semi-inverse points corresponding to C^+ lines with $\Delta M = 0.05$ at the corner. The downstream range of $y/x_c = 30$ was reached by about 600 (unequal) steps. The marching steps were limited in such a way that C^\pm trace points would not be more than one old grid interval apart. The SIMA and the exact results were compared by evaluating the relative difference in $M(o, y)$. We found that the relative error in Mach number increased from 0.1% at $y/x_c = 5$ [$M(o, y) = 3.8$] to 0.3% at $y/z_c = 30$ [$M(o, y) = 6.5$], which seems adequate for plume flow computations.

References

- ¹Zucrow, M. J., and Hoffman, J. D., *Gas Dynamics*, Wiley, New York, 1976.
- ²Liepmann, H. W., and Roshko, A., *Elements of Gasdynamics*, Wiley, New York, 1957.
- ³Falcovitz, J., "Numerical Computation of Ring-Symmetric Spacecraft Exhaust Plumes," Naval Postgraduate School, Monterey, CA, Rept. NPS 72-87-001CR, Jan. 1987.

Cylinder-Induced Shock-Wave Boundary-Layer Interaction

Oktay Özcan* and Bülent K. Yüceil†

Istanbul Technical University, Istanbul 80626, Turkey

Introduction

THE shock-wave boundary-layer interaction generated by a circular cylinder mounted on a flat plate is a problem of significant academic and practical importance. Korkegi¹ reports that such an interaction can cause structural damage on hypersonic aircraft. A detached bow shock wave is formed ahead of the cylinder. The boundary-layer developing on the flat plate interacts with the bow shock and separates. Sedney and Kitchens² and Özcan³ report that the number of separation lines ahead of the cylinder varies between one and three and is a strong function of the Reynolds number. Dolling and Bogdonoff⁴ report that the flowfields generated by circular cylinders and hemicylindrically blunted fins are very similar ahead of the protuberances. They also report that the protuberance height-to-diameter ratio is the relevant parameter for the generation of the asymptotic result, which occurs when increases in protuberance height do not change the interaction properties. Protuberances giving rise to the asymptotic result are called semi-infinite. The flow region upstream of the protuberances has received most of the attention in the previous studies of the flow. Dolling and Bogdonoff⁵ and Fomison and Stollery⁶ present some data for the downstream development of the flow in blunt-fin induced interactions. The report by Couch⁷ is probably the only reference presenting data for the development of the flow downstream of a cylinder.

This Note describes an experimental investigation of the shock-wave/turbulent boundary-layer interaction induced by a cylindrical protuberance at Mach numbers 1.7 and 2.2. Data are presented for flow regions both upstream and downstream of the cylinder. Various physical aspects of the flow are illuminated by the experimental data, which include the static pressure contours and the topology of the skin-friction lines on the flat plate. Yüceil⁸ gives a detailed description of the study and presentation of results.

Experiments

The experiments were carried out in the 60- × 30-mm transonic wind tunnel at the Istanbul Technical University in Turkey. This facility is a continuous tunnel operating at atmospheric stagnation conditions. The freestream Mach number M was varied by changing the shape of the Laval nozzle upstream of the test section. The freestream Reynolds number per meter length was 14.7×10^6 (1/m) and 12.0×10^6 (1/m) at Mach 1.7 and 2.2, respectively.

The circular cylinders used in the study were made of aluminum and were mounted on the centerline of the 60-mm-wide sidewall of the tunnel. The sidewall was perpendicular to the nozzle contour. The wetted length of the tunnel sidewall from

Received Feb. 14, 1991; revision received July 10, 1991; accepted for publication July 11, 1991. Copyright © 1991 by the American Institute of Aeronautics and Astronautics, Inc. All rights reserved.

*Associate Professor, Department of Aeronautics and Astronautics.

†Graduate Student, Department of Aeronautics and Astronautics; currently at University of Texas, Austin, TX 78712.

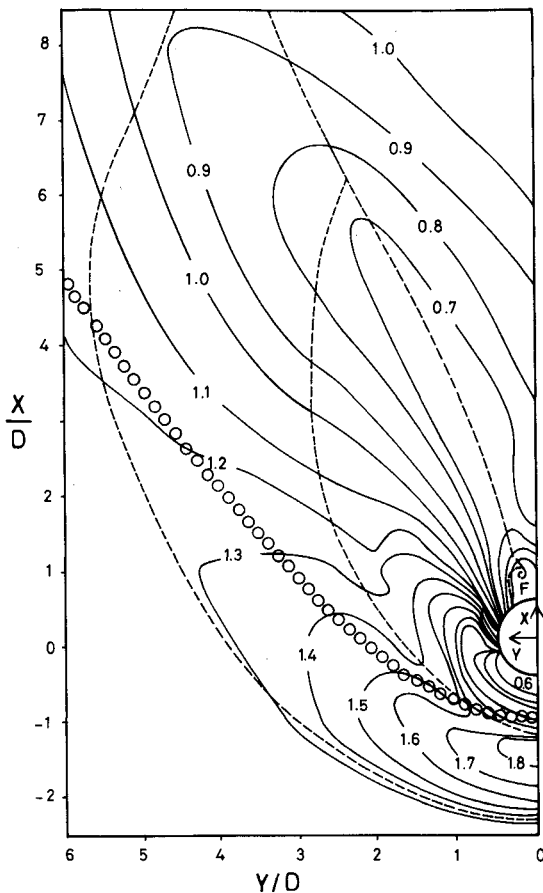


Fig. 1 Static pressure contours p/p_∞ for a semi-infinite cylinder ($D = 4$ mm, $H = 10$ mm) at Mach 2.2.

the nozzle throat was 40 cm. The calculated thickness of the turbulent, fully developed, undisturbed boundary layer on the tunnel sidewall was 7 ± 1 mm at Mach 1.7 and 2.2. The undisturbed skin-friction coefficient on the sidewall was 0.0022 and 0.0021 (± 0.0002) at Mach 1.7 and 2.2, respectively. These values of the skin-friction coefficient were calculated by using the Van Driest II transformation and the Sivells and Payne incompressible skin-friction formula.⁹ An adiabatic wall condition was assumed in the calculation. Results of Maisie and McDonald¹⁰ indicated that the ratio of momentum thickness to boundary-layer thickness was 0.080 and 0.073 at Mach 1.7 and 2.2, respectively, ahead of the interaction. The diameter D , height H , and height-to-diameter ratio H/D of the cylinders used in the study varied in the following ranges: $2 \leq D$ (mm) ≤ 16 , $4 \leq H$ (mm) ≤ 20 , $0.3 \leq H/D \leq 6.6$. The ratio of cylinder height to undisturbed boundary-layer thickness was between 0.5 and 2.5.

Oil flow visualization was made to observe the topology of the skin-friction line pattern on the flat plate. The separation distances were measured from the oil flow photographs taken during a tunnel run with an accuracy of ± 0.5 mm. Static pressures p on the flat plate were measured by a mercury manometer.

Discussion of Results

Figure 1 gives the static pressure contours p/p_∞ on the flat plate for a semi-infinite cylinder ($H = 10$ mm, $D = 4$ mm) at Mach 2.2. p_∞ is the undisturbed static pressure upstream of the interaction. The differences in the contour values is 0.2 immediately upstream of the cylinder and 0.1 elsewhere. The pressure contours upstream of the cylinder are qualitatively similar to the contours reported by Refs. 5 and 6 ahead of

blunt fins. The small circles denote the shape of the inviscid bow shock for an infinitely long cylinder. The shock shape was determined by an approximate method proposed in Ref. 11. Figure 1 also shows the X - Y Cartesian coordinate system chosen for data presentation. The dashed lines denote the oil accumulation lines, which are interpreted as separation lines. There exist two separation lines originating ahead of the cylinder and a pair of separation lines forming downstream of the cylinder. Note that only one half of the symmetry plane is shown in Fig. 1. The axis of symmetry is a line of reattachment downstream of the cylinder. The separation line originating downstream of the cylinder is probably due to the trailing shock wave reported by McCarthy and Kubota¹² in the wake of infinitely long cylinders. This separation line originates from the plate-cylinder junction, passes through the focus point F , and extends downstream. Sedney and Kitchens² report that point F is the footprint of a tornado vortex that, upon rising from the surface of the plate along the cylinder, bends downstream and becomes a longitudinal vortex embedded in the flat-plate boundary layer. In Fig. 1, the sidewall interference first occurs around $X/D = 4$ and $Y/D = 5$, where the primary separation line and the inviscid shock intersect each other. The interference effect is clearly evident on the separation line, which is deflected toward the symmetry plane for $X/D > 5$. The wall effects are probably confined to a small rectangle defined by $X/D > 4$ and $Y/D > 4.5$ in Fig. 1.

The qualitative nature of the skin-friction pattern and static pressure contours shown in Fig. 1 remained basically the same for all models and flow conditions of the study. A bifurcation occurred at low H/D ratios ($H/D < 1$), which modified the near wake region of the flow. A similar bifurcation is also reported by Sedney and Kitchens.² Figure 2 shows the static pressure contours (for positive Y) and the skin-friction line pattern (for negative Y) in the wake region of a finite cylinder

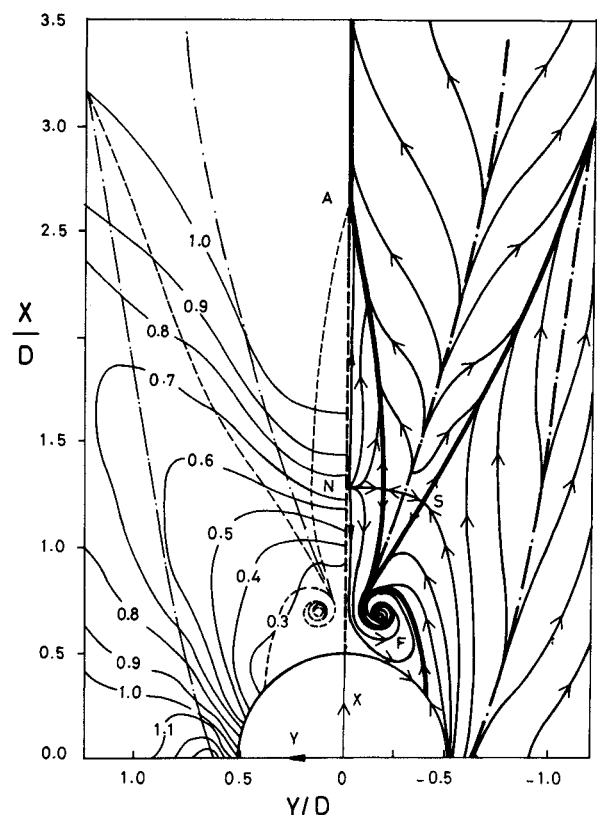


Fig. 2 Static pressure contours p/p_∞ (for $Y > 0$) and surface skin-friction lines (for $Y < 0$) for a finite cylinder ($D = 10$ mm, $H = 5$ mm) at Mach 2.2.

with $H/D = 0.5$ ($H = 5$ mm, $D = 10$ mm) at Mach 2.2. Separation lines are shown by thick lines. The dotted lines denote the reattachment lines whose shapes may be inaccurate due to difficulties in their observation. There exists an extra pair of separation and reattachment lines emanating downstream of the cylinder. One pair of separation lines diverge from the axis of symmetry as they extend downstream. The other pair converge and join each other at point A around $X/D = 2.5$. The latter pair are connected by a reattachment line that passes through the nodal and saddle singular points N and S. Özcan³ reports the existence of two pairs of separation lines that form downstream of the cylinder and both diverge from the axis of symmetry for the case of a laminar boundary layer at Mach 2.4. Figure 2 shows that the axis of symmetry, which is a reattachment line between the cylinder and point A, becomes a separation line downstream of point A. The reattachment line originating from point F diverges from the axis of symmetry as it extends downstream. It can be argued that this reattachment line is caused by the tornado vortex.

Figure 3 gives the variation of the normalized static pressure p/p_∞ along the axis of symmetry for various cylinders at Mach 2.2. Note that the scale of p/p_∞ is different upstream and downstream of the cylinders. The upstream pressure distributions in Fig. 3 indicate that the asymptotic result is obtained when $H/D \geq 2$. However, the pressure distributions downstream of the cylinders show that the cylinders become semi-infinite when $H/D \geq 2.5$. Thus, the downstream data impose a stricter limit for the definition of the asymptotic result.

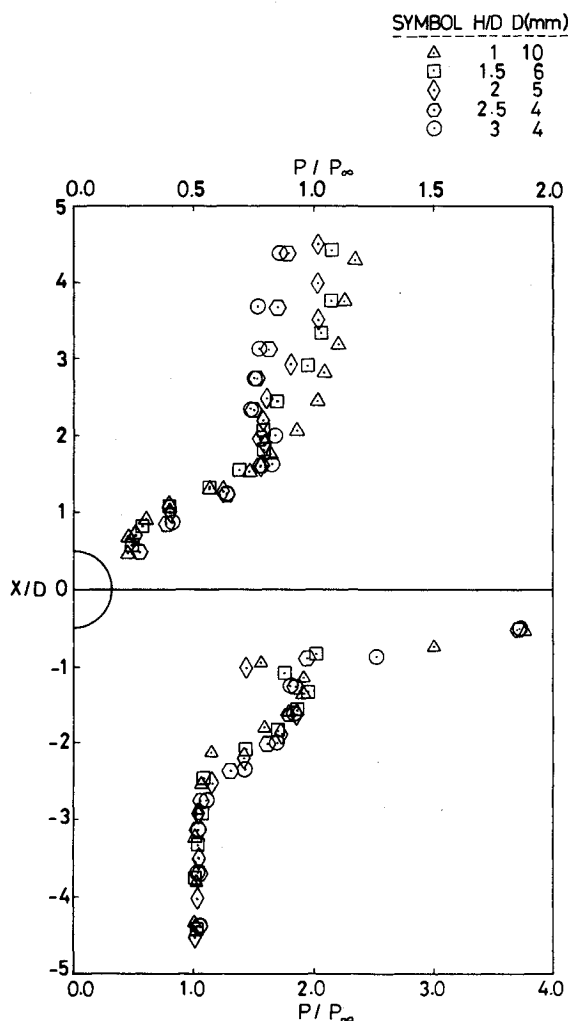


Fig. 3 Static pressure distributions p/p_∞ on the axis of symmetry for various cylinders at Mach 2.2.

Sedney and Kitchens¹³ propose the following correlation for the normalized primary separation distance S_1/D

$$S_1/D = \alpha (1 - e^{-\beta H/D})$$

where S_1 is measured along the axis of symmetry between the primary separation line and cylinder leading edge, and α and β are functions of the Mach number. They find $\alpha = 2.3$, $\beta = 1.50$ at Mach 3.5 and $\alpha = 2.2$, $\beta = 1.25$ at Mach 2.5. The values of α and β determined by the present study correlate the data with an accuracy of 15%. These values are $\alpha = 2.2$, $\beta = 1.15$ at Mach 2.2 and $\alpha = 2.5$, $\beta = 0.95$ at Mach 1.7. Data of the present study and Ref. 13 show that coefficient β increases monotonically with increasing M . This variation indicates that shorter cylinders become semi-infinite as Mach number increases. Shock standoff distance d/D was calculated by using an empirical relation proposed by Amick¹⁴: d/D values are 0.55 and 1.20 for Mach numbers 2.2 and 1.7, respectively. The observed increase of α as M decreases from 2.2 to 1.7 may be due to the increase in the shock standoff distance. The asymptotic value of the secondary separation distance S_2/D was found to be 0.95 and 0.80 at $M = 1.7$ and 2.2, respectively. Özcan³ reports an asymptotic S_2/D value of 1.5 for the case of a laminar boundary layer at $M = 2.4$.

Acknowledgments

This study was supported by the Institute of Science and Technology of the Istanbul Technical University.

References

- Korkegi, R., "Survey of Viscous Interactions Associated with High Mach Number Flight," *AIAA Journal*, Vol. 9, No. 5, 1971, pp. 771-784.
- Sedney, R., and Kitchens, C. W., "The Structure of Three Dimensional Separated Flows in Obstacle, Boundary-Layer Interactions," *AGARD Conference Proceedings*, AGARD 168, Göttingen, Germany, 1976.
- Özcan, O., "An Experimental Investigation of Three-Dimensional Boundary-Layer Separation in Supersonic Flow Past a Circular Cylinder on a Flat Plate," Ph.D. Dissertation, Univ. of California, Berkeley, CA, 1982.
- Dolling, D. S., and Bogdonoff, S. M., "Scaling of Interactions of Cylinders with Supersonic Turbulent Boundary Layers," *AIAA Journal*, Vol. 19, No. 5, 1981, pp. 655-657.
- Dolling, D. S., and Bogdonoff, S. M., "Blunt Fin-Induced Shock Wave Turbulent Boundary-Layer Interaction," *AIAA Journal*, Vol. 20, No. 12, 1982, pp. 1674-1680.
- Fomison, N. R., and Stollery, J. L., "The Effects of Sweep and Bluntness on Glancing Shock Wave Turbulent Boundary Layer Interaction," *AGARD Conference Proceedings*, AGARD 428, Bristol, UK, 1987.
- Couch, C. M., "Flow Field Measurements Downstream of Two Protuberances on a Flat Plate Submerged in a Turbulent Boundary Layer," NASA TN D-5297, July 1969.
- Yücelil, B. K., "An Experimental Investigation of Shock-Wave/Boundary-Layer Interaction Induced by Cylindrical Obstacles," M.S. Thesis, Istanbul Technical Univ., Istanbul, Turkey, 1989.
- Hopkins, E. J., and Inouye, M., "An Evaluation of Theories for Predicting Turbulent Skin Friction and Heat Transfer on Flat Plates at Supersonic and Hypersonic Mach Numbers," *AIAA Journal*, Vol. 9, No. 6, 1971, pp. 993-1003.
- Maise, G., and McDonald, H., "Mixing Length and Kinematic Eddy Viscosity in a Compressible Boundary Layer," *AIAA Journal*, Vol. 6, No. 1, 1968, pp. 73-80.
- Moeckel, W. E., "Approximate Method for Predicting Form and Location of Detached Shock Waves Ahead of Plane or Axially Symmetric Bodies," NASA TN-1921, July 1949.
- McCarthy, J. F., and Kubota, T., "A Study of Wakes Behind a Circular Cylinder at $M = 5.7$," *AIAA Journal*, Vol. 2, No. 4, 1964, pp. 629-636.
- Sedney, R., and Kitchens, C. W., "Separation Ahead of Protuberances in Supersonic Turbulent Boundary Layers," *AIAA Journal*, Vol. 15, No. 4, 1977, pp. 546-552.
- Amick, J. L., "Pressure Measurements on Sharp and Blunt 5 and 15 Degree Half-Angle Cones at Mach Number 3.86 and Angles of Attack to 100 Degrees," NASA TN D-753, Feb. 1961.